

# Potential Dependence of Electron-Transfer Rates at the Interface between Two Immiscible Electrolyte Solutions: Reduction of 7,7,8,8-Tetracyanoquinodimethane in 1,2-Dichloroethane by Aqueous Ferrocyanide Studied with Microelectrochemical Techniques

Jie Zhang and Patrick R. Unwin\*

Department of Chemistry, University of Warwick, Coventry CV4 7AL, U.K.

Received: September 21, 1999; In Final Form: November 6, 1999

Experimental studies of electron-transfer (ET) reactions at the interface between two immiscible electrolyte solutions (ITIES) were carried out with  $\text{Fe}(\text{CN})_6^{4-}$  as a reductant in water and 7,7,8,8-tetracyanoquinodimethane as an electron acceptor in 1,2-dichloroethane (DCE). The kinetics of this process have been determined using both scanning electrochemical microscopy and microelectrochemical measurements at expanding droplets.  $\text{ClO}_4^-$  was employed in each phase to control the interfacial potential drop. The ET rate constants were found to depend on the interfacial potential drop, with an apparent ET coefficient in the range 0.30–0.41 with a moderate aqueous ionic strength 0.1–0.3 M and an electrolyte concentration in the DCE phase of 0.1 M. When the aqueous ionic strength was increased significantly to the levels employed in studies of externally polarized ITIES, the ET rate constant decreased appreciably and was less dependent on the interfacial potential drop. These latter studies yielded results comparable to those obtained at externally polarized ITIES.

## Introduction

There is a great deal of interest in the study of electron-transfer (ET) reactions at the interface between two immiscible electrolyte solutions (ITIES) owing to the wide range of possible applications and fundamental significance.<sup>1</sup> ET between redox species confined to two immiscible solvents was first demonstrated more than 20 years ago,<sup>2</sup> and different theoretical treatments for this process have since been proposed. The contribution of solvent to the reorganization energy was calculated using models in which the interface was represented as a sharp boundary between two dielectrics.<sup>3,4</sup> In these models, most of the interfacial potential drop occurred between the reacting redox species across the ITIES. In an alternative approach, the formalism for homogeneous ET reactions was extended to the ITIES,<sup>5</sup> with the interface represented as a mixed solvent area. The interfacial potential difference had two contributions to the ET reaction: changing the ET Gibbs energy and the interfacial concentration of reactants. A similar interfacial structure was assumed in a model developed recently by Schmickler,<sup>6</sup> in which the potential drop between the reactants was small and effectively independent of the applied potential in solutions with relatively low ionic strength. Senda et al. described another theory,<sup>7</sup> in which the electrical double layer consisted of an inner layer sandwiched between two diffuse layers on each side of the interface, and the charge-transfer reaction occurred at the planes of contact of the inner layer with the two diffuse layers.

Experimental studies of ET kinetics at liquid/liquid interfaces are now appearing, which are able to test some of the elements outlined above. The Galvani potential difference ( $\Delta\phi_w$ ) between water (w) and an organic solvent (o) can be controlled in three different ways: by means of the equilibrium partitioning of a salt (nonpolarizable ITIES), by the partitioning of a single potential-determining ion, or via a potential supplied externally (ideally polarizable ITIES).<sup>8</sup>

Most of the early experimental results on the potential dependence of ET reactions at ITIES were obtained at externally polarized interfaces. In these studies, very high concentrations of supporting electrolyte were generally applied in the aqueous phase to salt out the organic electrolyte. Schiffrin and co-workers used cyclic voltammetry to study interfacial ET,<sup>9</sup> employing the Nicholson method<sup>10</sup> to extract standard rate constants. In an earlier paper,<sup>11</sup> the conventional theory of faradic impedance and the Butler–Volmer equation were applied to study ET at ITIES. However, the measured transfer coefficient was found to be potential dependent, which was attributed to double-layer effects and ionic adsorption.

Samec et al.<sup>12</sup> found that the rate constant for ET between ferrocene in nitrobenzene and aqueous ferricyanide was almost potential independent, but the studies were complicated by the transfer of ferrocenium ion from the organic phase to the aqueous phase. Girault et al.<sup>13</sup> studied the ET reaction between both 7,7,8,8-tetracyanoquinodimethane (TCNQ) and  $\text{Fe}(\text{CN})_6^{4-}$  and 1,1'-dimethylferrocene and  $\text{Fe}(\text{CN})_6^{3-}$  at a polarized water/1,2-dichloroethane (DCE) interface using in situ UV–visible spectroscopy. They found that the potential dependence of the observed rate constant did not show a purely Butler–Volmer trend.

Experimental studies have recently appeared using potential-determining ions to control the interfacial potential drop. Bard and co-workers<sup>14</sup> have pioneered the scanning electrochemical microscopy (SECM) approach, where the ET rate constants were measured without the interferences of  $iR$  drop and charging current, using  $\text{ClO}_4^-$  in each phase as a potential-determining ion. In most studies, a cationic oxidant 5,10,15,20-tetraphenyl-21H,23H-porphine zinc ( $\text{ZnPor}^+$ ) was generated in the organic phase by oxidation of the neutral species ( $\text{ZnPor}$ ) at the SECM tip electrode.  $\text{ZnPor}^+$  diffused to the ITIES where it was reduced to  $\text{ZnPor}$  by reaction with  $\text{Ru}(\text{CN})_6^{4-}$  or  $\text{Fe}(\text{CN})_6^{4-}$ . The measured electron-transfer coefficient was about 0.5 when the driving force was not too high, and the rate leveled off to a diffusion-controlled value at larger overpotentials.

\* Corresponding author. Email: P.R.Unwin@warwick.ac.uk.

Barker et al.<sup>15</sup> studied the reaction between  $\text{ZnPor}^+$  in benzene or benzonitrile and  $\text{Fe}(\text{CN})_6^{4-}$ ,  $\text{Ru}(\text{CN})_6^{4-}$ ,  $\text{Mo}(\text{CN})_8^{4-}$ , or  $\text{FeEDTA}^{2-}$  in the aqueous phase, using  $\text{ClO}_4^-$  as a potential-determining ion. A new SECM feedback model, which allowed the use of arbitrary concentrations of redox species in each phase, was applied to extract ET rate constants from the experimental results. An outcome of this research was a methodology that extended the upper range of rate constants accessible to study with SECM. The rate constants measured followed a trend with driving force consistent with Marcus theory.

Hitherto, experiments with externally polarized interfaces and potential-determining ions have been made on different redox systems. In this paper, we attempt to bridge this gap, using both SECM and microelectrochemical measurements at expanding droplets (MEMED), with the potential established with  $\text{ClO}_4^-$ , to measure ET rates on a system widely studied with techniques employing externally polarized ITIES.<sup>11,13,16,17</sup>  $\text{Fe}(\text{CN})_6^{4-}$  was applied in the aqueous phase, and TCNQ was selected as the organic electron acceptor, because the half-wave potential for  $\text{TCNQ}^-$  ion transfer from DCE to water is 0.2 V more positive than for ET from  $\text{Fe}(\text{CN})_6^{4-}$  to TCNQ.<sup>16</sup> This means that the measured kinetics will not be compromised by  $\text{TCNQ}^-$  transfer from DCE to the aqueous phase.

The use of TCNQ as one of the reactants is also interesting, because according to Schmickler's model<sup>6</sup> the concentration of a neutral species such as TCNQ at the ITIES should be potential independent. This avoids possible complications from interfacial concentration effects<sup>6</sup> in the organic phase. Because most of the interfacial potential drop occurs in the organic phase,<sup>18</sup> the  $\text{Fe}(\text{CN})_6^{4-}$  concentration at the ITIES should not change greatly, as suggested by Girault et al. in their recent studies.<sup>13</sup>

In the studies in this paper, different THAP concentrations have been employed in the DCE phase to study the effect of the organic electrolyte concentration on the ET reaction. Likewise, different concentrations of NaCl and  $\text{Li}_2\text{SO}_4$  have been used as the aqueous supporting electrolyte to investigate a range of conditions, including some that are close to the "salting out" protocols employed in earlier investigations of externally polarized interfaces.

In addition to SECM measurements, MEMED has been used for the first time to study ET kinetics at the ITIES. MEMED is a powerful new technique for the study of reactions that occur at liquid/liquid interfaces,<sup>19</sup> especially since it is very sensitive to the measurement of low reaction rates as compared to SECM. The present report shows that the reaction rate constants measured by SECM and MEMED are comparable in the region where both techniques are applicable. However, MEMED can be used to determine low ET rates that can barely be measured by SECM.

## Experimental Section

**Chemicals.**  $\text{Na}_4\text{Fe}(\text{CN})_6 \cdot 12\text{H}_2\text{O}$  (A.R., Strem), TCNQ (98%, Lancaster), tetra-*n*-hexylammonium perchlorate (THAP, crystalline, Alfa), NaCl (A.R., Fisons),  $\text{NaClO}_4 \cdot x\text{H}_2\text{O}$  (A.R.),  $\text{Li}_2\text{SO}_4 \cdot \text{H}_2\text{O}$  (99%), and DCE (HPLC grade) (Sigma-Aldrich) were used as received. All aqueous solutions were prepared from Milli-Q reagent water (Millipore Corp.).

**Electrodes and Electrochemical Cells.** All electrochemical measurements were made using a two-electrode arrangement. A saturated calomel electrode (SCE) served as the reference electrode, and a glass-coated Pt ultramicroelectrode (UME, 2 or 25  $\mu\text{m}$  diameter) functioned as the working electrode tip. The UME had a defined  $R_G$  value of 10 for SECM measure-

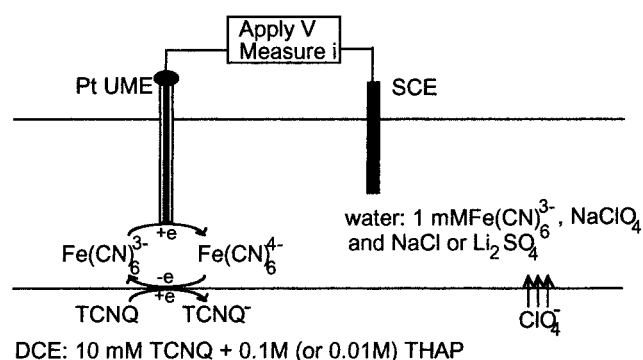


**Figure 1.** Schematic of the application of SECM in the measurement of ET reactions at ITIES.

ments and less than 4 for MEMED measurements.  $R_G = r_s/a$ , where  $r_s$  is the overall radius of the tip end (electrode plus insulating sheath) and  $a$  is the electrode radius. The electrodes were fabricated and polished as described previously.<sup>19,20</sup>

To measure the heterogeneous rate constants for the reaction between  $\text{Fe}(\text{CN})_6^{4-}$  and TCNQ using the SECM technique, a flat interface was established, in a conventional cell,<sup>20,21</sup> between an aqueous (top) phase and a DCE (bottom) phase. The aqueous phase contained 1 mM  $\text{Fe}(\text{CN})_6^{3-}$ , 0.1 M NaCl (or 0.1 M  $\text{Li}_2\text{SO}_4$ ), and 0.01–0.25 M  $\text{NaClO}_4$ , while the DCE phase contained 10 mM TCNQ and 0.1 M THAP.

For the MEMED technique, DCE droplets were formed periodically from a capillary submerged in an aqueous phase. The DCE phase contained 10 mM TCNQ and 0.01 (or 0.1) M THAP, while the aqueous receptor phase contained 1 mM  $\text{Fe}(\text{CN})_6^{4-}$ , with a supporting electrolyte that was either 0.1 or 2 M NaCl or 0.5 M  $\text{Li}_2\text{SO}_4$ , together with 0.01–0.25 M  $\text{NaClO}_4$ .

$\text{ClO}_4^-$  was the only ion common to both phases in all experiments. The electroneutrality of both phases was maintained by the transfer of this common ion when ET reactions occurred at the ITIES. The ratio of the bulk concentrations (strictly activities) of  $\text{ClO}_4^-$  in the aqueous and organic phases,  $[\text{ClO}_4^-]_w/[\text{ClO}_4^-]_o$ , determined the interfacial potential drop.

**Apparatus and Procedures.** The basic apparatus used for SECM and MEMED experiments has been described previously.<sup>19–21</sup> For the SECM measurements, a 25- $\mu\text{m}$ -diameter tip electrode was positioned in the top aqueous phase and biased at a potential where the reduction of  $\text{Fe}(\text{CN})_6^{3-}$  to  $\text{Fe}(\text{CN})_6^{4-}$  was diffusion-controlled. Approach curves were obtained by moving the tip toward the ITIES and recording the current as a function of  $d$  (the distance between the tip and the ITIES). There was generally a plateau in the current when the tip attained the distance of closest approach to the interface. Typically, a 25- $\mu\text{m}$ -diameter tip could be approached to a distance of ca. 1–2  $\mu\text{m}$  from the liquid/liquid interface. To determine this distance precisely, experiments were always run without any TCNQ in the DCE phase and data analyzed with negative feedback theory similar to that of Kwak and Bard.<sup>22</sup> For ET measurements, the tip electrode generated  $\text{Fe}(\text{CN})_6^{4-}$ , which diffused to the ITIES where it was oxidized back to  $\text{Fe}(\text{CN})_6^{3-}$  by the reaction with TCNQ, producing  $\text{TCNQ}^-$  in the organic phase (see Figure 1).

In MEMED measurements, a DCE drop containing TCNQ was grown from a capillary with an internal diameter of about 200  $\mu\text{m}$ . Amperometric detection was used, and the tip current for the species of interest was recorded as a function of time when the drop grew toward the tip (see Figure 2). In contrast to SECM, the small size of the tip (2  $\mu\text{m}$  diameter) used for these measurements ensured that the electrode was a noninvasive

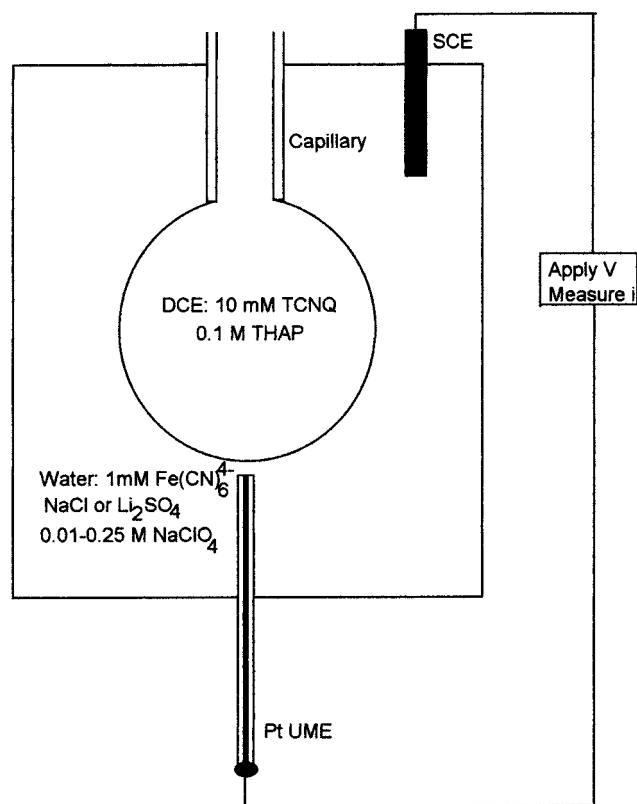


**Figure 2.** Schematic of the application of MEMED in the measurement of ET reactions at ITIES.

probe of the concentration boundary layer that developed adjacent to the droplet. A method for obtaining the time-dependent droplet concentration profile from the UME response has been outlined fully elsewhere.<sup>19b</sup> The distance at which the tip contacted the ITIES was taken as the point where the tip current changed suddenly on reaching the interface.

## Results and Discussion

**Potential Drop across the ITIES.** The relative values of the potential drop across the liquid/liquid interface were obtained by adopting the procedure advocated by Bard and co-workers.<sup>14c</sup> Steady-state linear sweep voltammograms for the reduction of TCNQ at a 25- $\mu\text{m}$ -diameter microdisk electrode in DCE solution were measured with respect to an SCE positioned in an aqueous phase. The reversible half-wave potential was derived from these voltammograms.

If activities are approximated by concentrations,  $\Delta^\circ_w\phi$  at the DCE/aqueous liquid junction in this experiment should be governed by the concentration ratio of the potential-determining ion,  $\text{ClO}_4^-$ , in water and DCE. At standard temperature and pressure, the following equation should hold<sup>14c</sup>

$$\Delta^\circ_w\phi^\circ = \Delta^\circ_w\phi^\circ_{\text{ClO}_4^-} - 0.059 \log \frac{[\text{ClO}_4^-]_w}{[\text{ClO}_4^-]_o} \quad (1)$$

where  $\Delta^\circ_w\phi^\circ_{\text{ClO}_4^-}$  is the standard transfer potential of  $\text{ClO}_4^-$ . If  $[\text{ClO}_4^-]_o$  is maintained constant, the formal (strictly, standard) potential of an electrochemical reaction at an electrode in DCE, measured with respect to the aqueous reference electrode, should shift by 59 mV to more negative values with a decade increase in  $[\text{ClO}_4^-]_w$ .

A typical steady-state voltammogram of TCNQ reduction obtained at a 25- $\mu\text{m}$ -diameter Pt UME is shown in Figure 3.

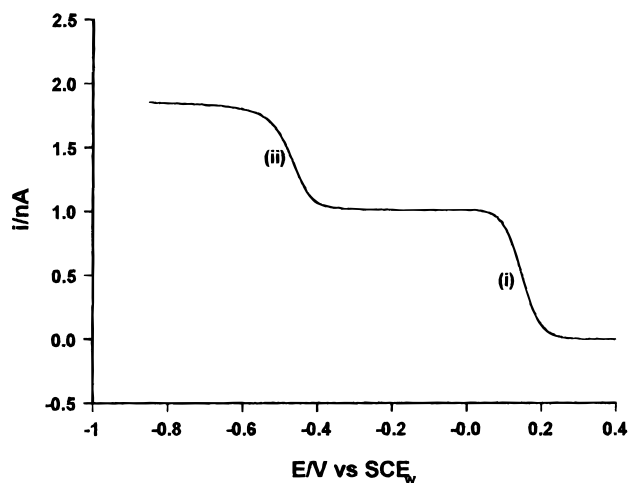


**Figure 3.** Steady-state voltammogram for TCNQ reduction in DCE at a 25- $\mu\text{m}$ -diameter Pt UME. The DCE solution contained 0.2 mM TCNQ and 0.01 M THAP. An SCE was placed in the aqueous solution containing 0.1 M NaCl and 0.01 M  $\text{NaClO}_4$ .

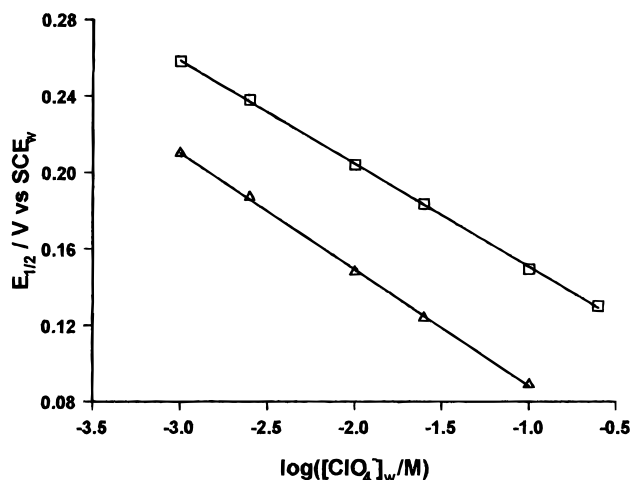


**Figure 4.** Dependence of the half-wave potentials for the reversible first reduction of TCNQ in DCE on  $[\text{ClO}_4^-]_w$ , with  $[\text{THAP}]_o = 0.1$  M ( $\square$ ) or 0.01 M ( $\triangle$ ).

Two well-defined waves corresponding to two one-electron reductions of TCNQ to  $\text{TCNQ}^-$  (wave i) and then to  $\text{TCNQ}^{2-}$  (wave ii) are evident. From the plateau current, the diffusion coefficient of TCNQ was  $1.05 \times 10^{-5} \text{ cm}^2 \text{ s}^{-1}$  when 0.01 M THAP was used as the supporting electrolyte in the DCE phase. This value was calculated using eq 2.

$$i_{\text{lim}} = 4nFDaC \quad (2)$$

where  $i_{\text{lim}}$  is the steady-state limiting current,  $n$  is the number of electrons transferred,  $F$  is Faraday's constant,  $D$  is the diffusion coefficient, and  $C$  is the bulk concentration of TCNQ.

The dependence of the half-wave potential ( $E_{1/2}$ ) of the first reduction of TCNQ in DCE on  $[\text{ClO}_4^-]_w$ , deduced from measurements such as those in Figure 3, is shown in Figure 4 for two  $[\text{THAP}]_o$ . The slopes of the straight lines agree well with the predictions of eq 1. Although the ionic strength of the aqueous phase changes in these measurements, the activity coefficients of the various aqueous ions are likely to be fairly insensitive to the ionic strength for the range of these experiments and those that follow.<sup>23</sup> It is further worth noting that while  $E_{1/2}$  depends on  $[\text{ClO}_4^-]_w$ , it was found to be almost independent of the ionic strength in the aqueous phase for the

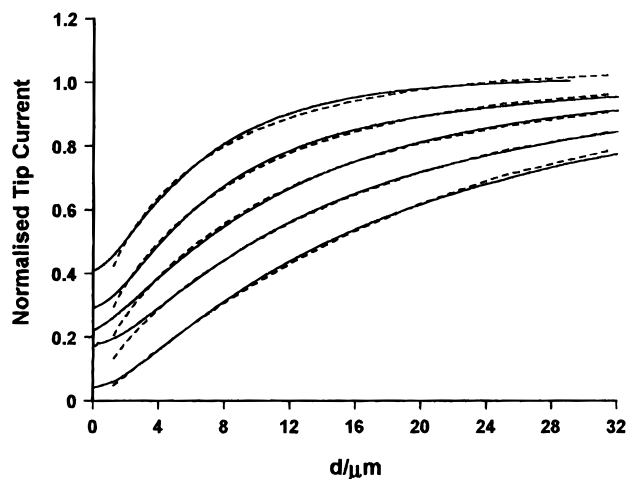


**Figure 5.** Dependence of ET rates on  $[\text{ClO}_4^-]_w$ , with  $[\text{THAP}]_o = 0.1$  M fixed. The SECM approach curves were obtained with a 25- $\mu\text{m}$ -diameter Pt UME. From top to bottom, the first four solid experimental curves are shown for  $[\text{ClO}_4^-]_w = 0.010, 0.025, 0.10$ , and  $0.25 \text{ mol dm}^{-3}$ . For the bottom solid line,  $[\text{ClO}_4^-]_w = 0.1$  M, there was no TCNQ in the DCE phase. The corresponding dashed theoretical curves are shown for  $k = 0.15, 0.08, 0.04, 0.015$ , and  $0 \text{ cm s}^{-1} \text{ M}^{-1}$ .

concentration range of inert electrolyte applied in our experiments (defined later).

**Potential Dependence of ET Rates.** SECM measurements of the rate constants of ET between TCNQ in the DCE phase and  $\text{Fe}(\text{CN})_6^{4-}$  in the aqueous phase were carried out using  $\text{ClO}_4^-$  as the potential-determining ion, as outlined in the Experimental Section. Typical results are shown in Figure 5, where  $d$  is the distance between the tip and the ITIES. In this figure, the normalized tip current is the ratio of the measured steady-state current at  $d$  to that measured at  $d \rightarrow \infty$ . The rate constant,  $k_f$  ( $\text{cm s}^{-1}$ ) is the apparent heterogeneous rate constant, and  $k = k_f/[\text{TCNQ}]$  ( $\text{cm s}^{-1} \text{ M}^{-1}$ ) is the effective bimolecular rate constant. Comparing the data in Figures 4 and 5, it can be seen that as  $[\text{ClO}_4^-]_w$  increases, the interfacial potential drop (and thus driving force) for ET at the ITIES decreases. This is manifested as a decrease in the measured values of  $k$  with increasing  $[\text{ClO}_4^-]_w$ . Any possible complications due to the changes in the ionic strength in the aqueous phase, in these and related experiments, were ruled out with control experiments in which the concentration of  $\text{NaClO}_4$  was fixed at 0.1 M and the concentration of  $\text{NaCl}$  increased from 0 to 0.2 M.

The rate constants of ET between TCNQ and  $\text{Fe}(\text{CN})_6^{4-}$  were also measured by the MEMED technique using  $\text{ClO}_4^-$  as the potential-determining ion. In this study,  $\text{Fe}(\text{CN})_6^{4-}$  (initial concentration 1 mM) was determined in the aqueous receptor phase, while forming a DCE droplet containing 10 mM TCNQ and 0.1 M THAP.  $\text{NaCl}$  (0.1 M) was applied in the aqueous phase together with various concentrations of  $\text{NaClO}_4$ . Typical concentration profiles for different  $[\text{ClO}_4^-]_w$  are shown in Figure 6. In this figure, the local concentration of  $\text{Fe}(\text{CN})_6^{4-}$  has been normalized with respect to the bulk solution value,  $[\text{Fe}(\text{CN})_6^{4-}]^*$ . The rate constants employed to fit the data are seen to be comparable to those measured by SECM (see Figure 5).

The data in Figures 5 and 6 clearly show that the ET rate constants depend on the interfacial potential drop, with  $k$  increasing with an increase in the driving force. The back-reaction between  $\text{TCNQ}^-$  and  $\text{Fe}(\text{CN})_6^{3-}$  was neglected in our analysis, even if the driving force was small, because there was always a high concentration of TCNQ in the DCE phase, compared to  $\text{Fe}(\text{CN})_6^{3-/4-}$  in the aqueous phase, and the

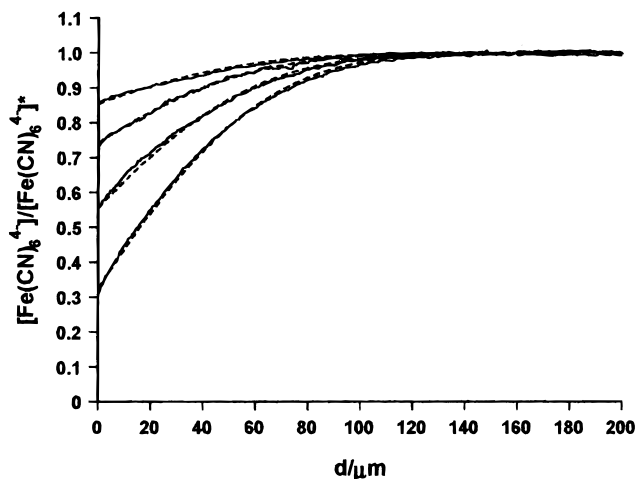


**Figure 6.** Normalized concentration profiles (solid lines) of  $\text{Fe}(\text{CN})_6^{4-}$  in the aqueous receptor phase ( $[\text{THAP}]_o = 0.1$  M), obtained using MEMED technology. Drop time and final size were 9.2 s and 0.99 mm. From bottom to top, the solid experimental curves are shown for  $[\text{ClO}_4^-]_w = 0.01, 0.025, 0.1$ , and  $0.25 \text{ M}$ , while the corresponding dashed curves (also bottom to top) are the theoretical behavior for  $k = 0.22, 0.09, 0.04$ , and  $0.02 \text{ cm s}^{-1} \text{ M}^{-1}$ .

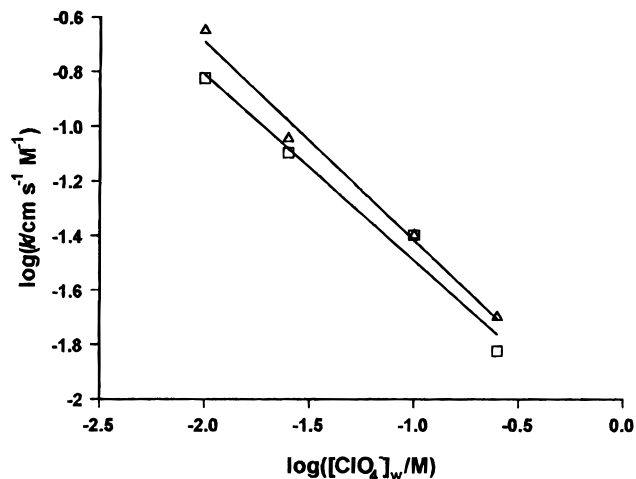


**Figure 7.** Dependence of  $k$  on the  $\text{ClO}_4^-$  concentration in the aqueous phase; the data are those from Figure 5 ( $\square$ ) and Figure 6 ( $\triangle$ ).

relatively small proportion of the product  $\text{TCNQ}^-$  diffuses away from the ITIES to the bulk DCE phase quickly.

With a fixed concentration of TCNQ, the dependence of ET rates on the driving force can be written as<sup>14c</sup>

$$k = \text{const} \exp(-\Delta G^\ddagger/RT) \quad (3)$$

where  $\Delta G^\ddagger$  is the free energy barrier. Because the experiments described here have been carried out with a relatively low driving force, previous SECM studies<sup>14c</sup> suggest that a Butler–Volmer type approximation could be used for the ITIES directly, so that

$$\Delta G^\ddagger = -\alpha F(\Delta E^\circ + \Delta \phi_w) \quad (4)$$

where  $\Delta E^\circ$  is the standard potential difference of the two redox couples ( $E_{\text{TCNQ}^-/\text{TCNQ}}^\circ - E_{\text{Fe}(\text{CN})_6^{3-/4-}}^\circ$ ),  $F$  is Faraday's constant, and  $\alpha$  is the transfer coefficient. For the two redox couples, the  $\Delta E^\circ$  value is fixed and the combination of eqs 3 and 4 yields

$$\log k = \text{const} - 0.06\alpha \log[\text{ClO}_4^-]_w/f \quad (5)$$



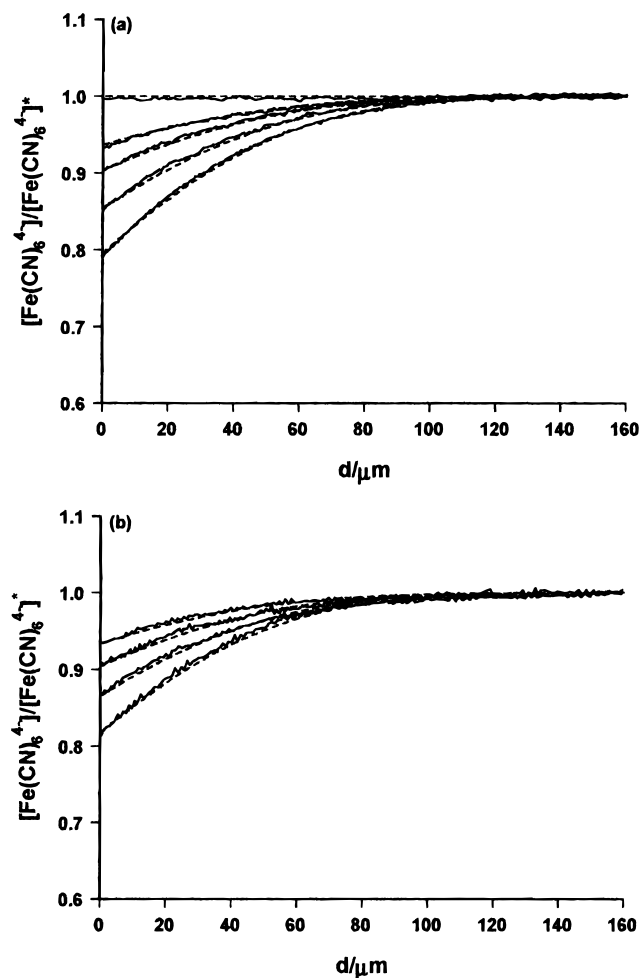


**Figure 8.** Normalized concentration profiles (solid lines) of  $\text{Fe}(\text{CN})_6^{4-}$  in the aqueous receptor phase, obtained using MEMED, with  $[\text{NaCl}]_w = 2 \text{ M}$ . Drop time and final size were 9.2 s and 0.99 mm. In (a)  $[\text{THAP}]_o = 0.1 \text{ M}$ , and the first four solid experimental curves (bottom to top) are shown for  $[\text{ClO}_4^-]_w = 0.01, 0.025, 0.1$ , and  $0.25 \text{ M}$ . For the top solid line, there was no TCNQ in the DCE phase, while the corresponding dashed curves are the theoretical behavior for  $k = 0.03, 0.02, 0.013, 0.008$ , and  $0 \text{ cm s}^{-1} \text{ M}^{-1}$ . In (b)  $[\text{THAP}]_o = 0.01 \text{ M}$ , and the solid experimental curves (bottom to top) are shown for  $[\text{ClO}_4^-]_w = 0.01, 0.025, 0.1$ , and  $0.25 \text{ M}$ , while the corresponding dashed curves are the theoretical behavior for  $k = 0.025, 0.0175, 0.012$ , and  $0.008 \text{ cm s}^{-1} \text{ M}^{-1}$ .

where  $f = RT/F$ . Thus, the  $\log k$  vs  $\log[\text{ClO}_4^-]_w$  dependence should be linear with a slope proportional to  $\alpha$ .

From the SECM measurements, the Tafel plot obtained for ET between  $\text{Fe}(\text{CN})_6^{4-}$  and TCNQ was linear with an apparent measured  $\alpha$  value of  $0.29 \pm 0.03$ , while the  $\alpha$  value measured by the MEMED technique was  $0.31 \pm 0.02$ . The data obtained from these two methods are plotted in Figure 7.

**Effect of Aqueous Ionic Strength on the ET reaction.** The effect of aqueous ionic strength was investigated by applying 2M NaCl in the aqueous phase, still using  $\text{ClO}_4^-$  as the potential-determining ion. MEMED technology was used in these studies owing to its high sensitivity to the low reaction rates that were found in these experiments, which were hardly measurable by SECM. THAP was employed at a concentration of either 0.1 or 0.01 M, together with 10 mM TCNQ in the DCE (droplet) phase.

Typical concentration profiles are shown in Figure 8, and the corresponding Tafel plots are in Figure 9. In comparison to the data in Figure 7, these results show that the ET rate constant decreases considerably and is less dependent on the interfacial

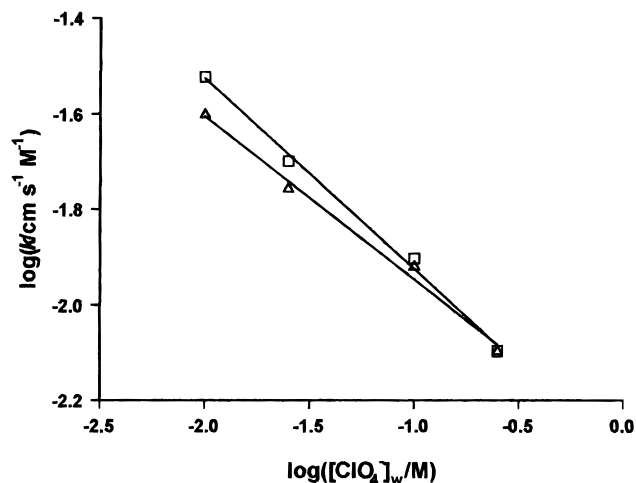


**Figure 9.** Dependence of  $k$  on the  $\text{ClO}_4^-$  concentration in the aqueous phase; the data are taken from parts a ( $\square$ ) and b ( $\triangle$ ) of Figure 8.

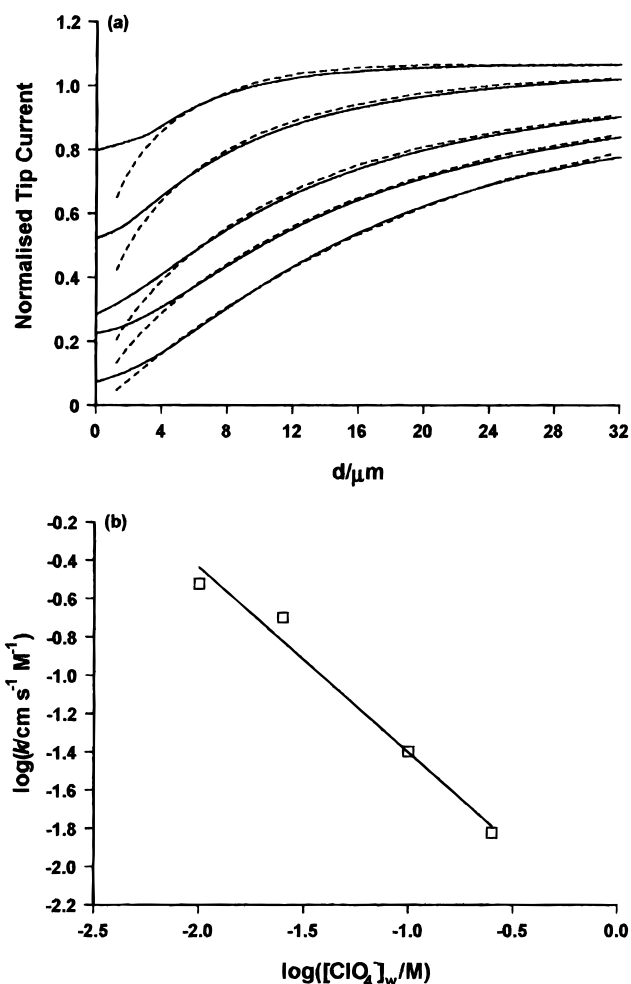


**Figure 10.** Dependence of  $k$  on  $\text{ClO}_4^-$  concentration in the aqueous phase, with  $[\text{Li}_2\text{SO}_4]_w = 0.1 \text{ M}$  and  $[\text{THAP}]_o = 0.1 \text{ M}$ . (a) SECM approach curves obtained with a  $25\text{-}\mu\text{m}$ -diameter Pt UME. From top to bottom, the first four solid experimental curves are shown for  $[\text{ClO}_4^-]_w = 0.01, 0.025, 0.1$ , and  $0.25 \text{ M}$ . For the bottom solid line, there was no TCNQ in the DCE phase. The dashed lines are the corresponding theoretical curves for  $k = 0.3, 0.2, 0.04, 0.015$ , and  $0 \text{ cm s}^{-1} \text{ M}^{-1}$ . (b) Tafel plot of the data in (a).

potential drop ( $\alpha = 0.17 \pm 0.01$  when  $[\text{THAP}] = 0.1 \text{ M}$  and  $0.14 \pm 0.01$  when  $[\text{THAP}] = 0.01 \text{ M}$ ). Similar effects were observed when  $\text{Li}_2\text{SO}_4$  was used as the supporting electrolyte in the aqueous phase. The measured  $\alpha$  value decreased from

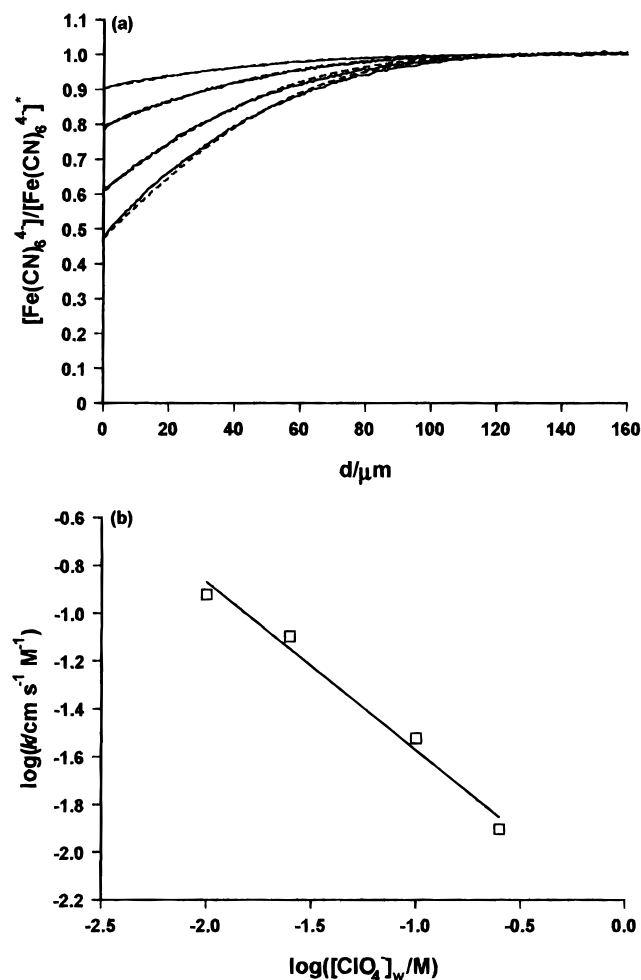


**Figure 11.** Dependence of  $k$  on  $\text{ClO}_4^-$  concentration in the aqueous receptor phase, with  $[\text{Li}_2\text{SO}_4]_w = 0.5 \text{ M}$  and  $[\text{THAP}]_o = 0.1 \text{ M}$ . (a) MEMED  $\text{Fe(CN)}_6^{4-}$  concentration profiles obtained with a  $2\text{-}\mu\text{m}$ -diameter Pt UME. From bottom to top, the solid experimental curves are shown for  $[\text{ClO}_4^-]_w = 0.01, 0.025, 0.1, \text{ and } 0.25 \text{ M}$ , and the dashed curves are the corresponding theoretical behavior for  $k = 0.12, 0.08, 0.03, \text{ and } 0.0125 \text{ cm s}^{-1} \text{ M}^{-1}$ . (b) Tafel plot of the data in (a).

$0.41 \pm 0.04$  (with  $[\text{THAP}]_o = 0.10 \text{ M}$  and  $[\text{Li}_2\text{SO}_4]_w = 0.10 \text{ M}$ ) to  $0.30 \pm 0.03$  (with  $[\text{THAP}]_o = 0.1 \text{ M}$  and  $[\text{Li}_2\text{SO}_4]_w = 0.50 \text{ M}$ ) and  $0.24 \pm 0.01$  (with  $[\text{THAP}]_o = 0.01 \text{ M}$  and  $[\text{Li}_2\text{SO}_4]_w = 0.50 \text{ M}$ ). Results from these different experiments are shown in Figures 10–12. The trend observed of lower rate constant with increasing  $\text{Li}_2\text{SO}_4$  concentration may be caused by the salting out effect, which is proposed to create a fairly rigid interfacial ion-free region.<sup>11</sup> If this increases the distance over which the potential drops in the organic phase, and a neutral reactant like TCNQ can penetrate this region, then this could explain the decrease in the  $k$  and  $\alpha$  values observed when conditions in the aqueous phase mimic those employed in studies with externally polarized ITIES.

The experimental conditions in Figure 12 are very close to those in Girault's report where the ITIES was polarized externally.<sup>13</sup> The  $\alpha$  value measured in this study is  $0.24 \pm 0.01$  and  $k$  is  $0.01 \text{ cm s}^{-1} \text{ M}^{-1}$  at  $E_{1/2} = 0.09 \text{ V}$ , for the reduction of TCNQ vs  $\text{SCE}_w$  with  $0.1 \text{ M NaClO}_4$  in the aqueous phase and  $0.01 \text{ M THAP}$  in the DCE phase. This corresponds to  $\Delta^w_o\phi = -0.11 \text{ V}$  when the potential scale is corrected against the standard transfer potential of  $\text{ClO}_4^-$  ( $-0.17 \text{ V}$ )<sup>1b</sup> using the known formal half-wave potential for the first reduction of TCNQ ( $0.22 \text{ V vs SHE}$ ).<sup>14b</sup> The effective  $\alpha$  value measured by Girault et al. was ca. 0.15 and  $k$  was  $0.005 \text{ cm s}^{-1} \text{ M}^{-1}$  when

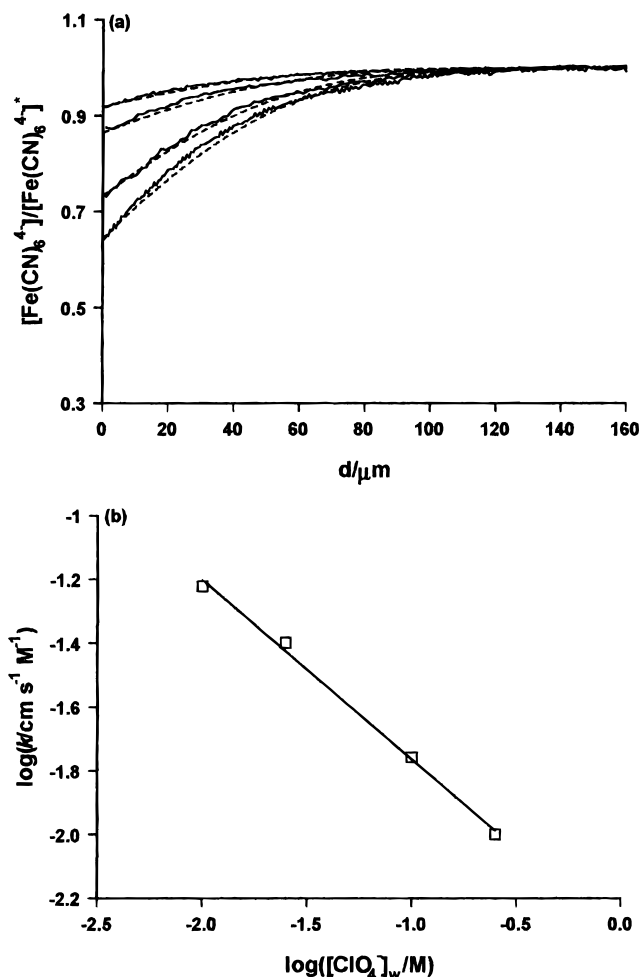


**Figure 12.** Dependence of  $k$  on  $\text{ClO}_4^-$  concentration in the aqueous receptor phase, with  $[\text{Li}_2\text{SO}_4]_w = 0.5 \text{ M}$  and  $[\text{THAP}]_o = 0.01 \text{ M}$ . (a) MEMED  $\text{Fe(CN)}_6^{4-}$  concentration profiles obtained with a  $2\text{-}\mu\text{m}$ -diameter Pt UME. From bottom to top, the solid experimental curves are shown for  $[\text{ClO}_4^-]_w = 0.01, 0.025, 0.1, \text{ and } 0.25 \text{ M}$ , and the dashed curves are the corresponding theoretical behavior for  $k = 0.06, 0.04, 0.0175, \text{ and } 0.01 \text{ cm s}^{-1} \text{ M}^{-1}$ . (b) Tafel plot of the data in (a).

$\Delta^w_o\phi = -0.11 \text{ V}$ . If the effects of some uncertain factors, for example, the precision of the quoted half-wave potential of the first reduction TCNQ and the standard transfer potential of  $\text{ClO}_4^-$ , are considered when converting the potential scale, then the results in Figure 12 are reasonably consistent with earlier studies on externally polarized interfaces.

## Conclusions

SECM and MEMED have been used to investigate the ET reaction between  $\text{Fe(CN)}_6^{4-}$  and TCNQ at the ITIES. The interfacial potential drop was adjusted by the potential-determining  $\text{ClO}_4^-$  ion. Comparable results were obtained using these two techniques. Moreover, the techniques complement each other rather well, as SECM is sensitive to the measurement of fast kinetic processes, while MEMED is more sensitive to slower processes.

The ET rate constants were found to depend on the interfacial potential drop, with an apparent measured ET coefficient in the range  $0.30\text{--}0.41$  when  $0.1 \text{ M NaCl}$  (or  $\text{Li}_2\text{SO}_4$ ) was employed in the aqueous phase, together with various concentrations of  $\text{NaClO}_4$ . An  $\alpha$  value in this range is certainly not inconsistent with Marcus theory, in which the effective value of  $\alpha$  is 0.5 in the limit of low driving force, decreasing with increasing driving

force to zero at the point where the inverted region starts and then taking on negative values at higher driving force still.<sup>15</sup>

The experimental results show that the ET rate constant decreased significantly and showed less dependence on the interfacial potential drop when 0.5 M Li<sub>2</sub>SO<sub>4</sub> or 2 M NaCl was applied as the supporting electrolyte in the aqueous phase. It has been suggested that the salting out procedure creates a fairly rigid interfacial ion-free region.<sup>11</sup> If this increases the distance over which the potential drops in the organic phase and a neutral reactant like TCNQ can penetrate this region, then this could explain both the decreased *k* and  $\alpha$  values observed when conditions in the aqueous phase mimic those employed in studies with externally polarized ITIES. More generally, our studies suggest that when the conditions are similar, measurements made at ITIES with potential-determining ions yield results that are reasonably comparable to those obtained at externally polarized ITIES.

Although our results show that the measured  $\alpha$  decreased slightly when the organic electrolyte concentration decreased from 0.1 to 0.01 M, the ionic strength in the system we studied is not low enough to test Schimikler's theory.<sup>6</sup> Further studies in this direction are necessary. Our investigations support the advocacy of Girault et al.<sup>13</sup> that the TCNQ/ferrocynide system is a good one for the investigation of electron-transfer kinetics at ITIES.

**Acknowledgment.** We thank the EPSRC (GR/L15074) and Zeneca for support. J.Z. also gratefully acknowledges scholarships from the ORS scheme and the University of Warwick. We appreciate helpful discussions with Anna L. Barker and Dr. Christopher J. Slevin (University of Warwick) and particularly thank them for providing programs for SECM and MEMED analysis. Fruitful discussions with Dr. John Atherton (Avecia, Process Technology, Huddersfield) on reactivity at liquid/liquid interfaces are greatly appreciated.

## References and Notes

- (1) (a) Volkov, A. G.; Deamer, D. W.; Tanelian, D. L.; Markin, V. S. *Liquid Interfaces in Chemistry and Biology*; Wiley: New York, 1998. (b) Girault, H. H.; Schiffrin, D. J. In *Electroanalytical Chemistry*; Bard, A. J., Ed.; Marcel Dekker: New York, 1989; Vol. 15, p 1.
- (2) Guainazzi, M.; Silvestry, G.; Survalle, G. *Chem. Commun.* **1975**, 200.
- (3) (a) Marcus, R. A. *J. Phys. Chem.* **1990**, *94*, 1050. (b) Marcus, R. A. *J. Phys. Chem.* **1990**, *94*, 4152; *J. Phys. Chem.* **1990**, *94*, 7742

- (addendum). (c) Marcus, R. A. *J. Phys. Chem.* **1991**, *95*, 2010; *J. Phys. Chem.* **1995**, *99*, 5742 (addendum).
- (4) (a) Kharkats, Yu. I.; Volkov, A. G. *J. Electroanal. Chem.* **1985**, *184*, 435. (b) Kharkats, Yu. I.; Ulstrup, J. *J. Electroanal. Chem.* **1991**, 308, 17.
  - (5) Girault, H. H. and Schiffrin, D. J. *J. Electroanal. Chem.* **1988**, 244, 15.
  - (6) Schmickler, W. *J. Electroanal. Chem.* **1997**, 428, 123.
  - (7) (a) Senda, M. *Anal. Sci.* **1994**, *10*, 649. (b) Senda, M. *Electrochim. Acta* **1995**, *40*, 2993. (c) Katano, H.; Maeda, K.; Senda, M. *J. Electroanal. Chem.* **1995**, 396, 391.
  - (8) Samec, Z. *Chem. Rev.* **1988**, *88*, 617.
  - (9) (a) Geblewicz, G.; Schiffrin, D. J. *J. Electroanal. Chem.* **1988**, 244, 27. (b) Cunnane, V. J.; Schiffrin, D. J.; Beltran, C.; Geblewicz, G.; Solomon, T. *J. Electroanal. Chem.* **1988**, 247, 203.
  - (10) Nicholson, R. S. *Anal. Chem.* **1965**, 37, 1351.
  - (11) Cheng, Y.; Schiffrin, D. J. *J. Chem. Soc., Faraday Trans.* **1993**, 89, 199.
  - (12) Samec, Z.; Marecek, V.; Weber, J.; Homolka, D. *J. Electroanal. Chem.* **1981**, 126, 105.
  - (13) Ding, Z.; Fermin, D. J.; Brevet, P. F.; Girault, H. H. *J. Electroanal. Chem.* **1998**, 458, 139.
  - (14) (a) Wei, C.; Bard, A. J.; Mirkin, M. V. *J. Phys. Chem.* **1995**, *99*, 43. (b) Solomon, T.; Bard, A. J. *J. Phys. Chem.* **1995**, *99*, 17487. (c) Tsionsky, M.; Bard, A. J.; Mirkin, M. V. *J. Phys. Chem.* **1996**, *100*, 17881. (d) Tsionsky, M.; Bard, A. J.; Mirkin, M. V. *J. Am. Chem. Soc.* **1997**, *119*, 10785. (e) Delville, M. H.; Tsionsky, M.; Bard, A. J. *Langmuir* **1998**, *14*, 2774.
  - (15) Barker, A. L.; Unwin, P. R.; Amemiya, S.; Zhou, J.; Bard, A. J. *J. Phys. Chem. B* **1999**, *103*, 7260.
  - (16) Cheng, Y.; Schiffrin, D. J. *J. Chem. Soc., Faraday Trans.* **1994**, *90*, 2517.
  - (17) (a) Dryfe, R. A. W.; Webster, R. D.; Coles, B. A.; Compton, R. G. *Chem. Commun.* **1997**, 779. (b) Ding, Z.; Brevet, P. F.; Girault, H. H. *Chem. Commun.* **1997**, 2059. (c) Webster, R. D.; Dryfe, R. A. W.; Coles, B. A.; Compton, R. G. *Anal. Chem.* **1998**, *70*, 792.
  - (18) Fermin, D. J.; Ding, Z. F.; Duong, H. D.; Brevet, P. F.; Girault, H. H. *J. Phys. Chem. B* **1998**, *102*, 10334.
  - (19) (a) Slevin, C. J.; Unwin, P. R. *Langmuir* **1997**, *13*, 4799. (b) Slevin, C. J.; Unwin, P. R. *Langmuir* **1999**, *15*, 7361. (c) Zhang, J.; Slevin, C. J.; Unwin, P. R. *Chem. Commun.* **1999**, 1501.
  - (20) (a) Macpherson, J. V.; Unwin, P. R. *J. Phys. Chem.* **1994**, *98*, 1704. (b) Macpherson, J. V.; Unwin, P. R. *J. Phys. Chem.* **1994**, *98*, 3109. (c) Macpherson, J. V.; Unwin, P. R. *J. Phys. Chem.* **1995**, *99*, 3338. (d) Macpherson, J. V.; Unwin, P. R. *J. Phys. Chem.* **1995**, *99*, 14824. (e) Macpherson, J. V.; Unwin, P. R. *J. Phys. Chem.* **1996**, *100*, 19475. (f) Macpherson, J. V.; Hiller, A. C.; Unwin, P. R.; Bard, A. J. *J. Am. Chem. Soc.* **1996**, *118*, 6445. (g) Barker, A. L.; Macpherson, J. V.; Slevin, C. J.; Unwin, P. R. *J. Phys. Chem. B* **1998**, *102*, 1586.
  - (21) (a) Slevin, C. J.; Umbers, J. A.; Atherton, J. H.; Unwin, P. R. *J. Chem. Soc., Faraday Trans.* **1996**, *92*, 5177. (b) Slevin, C. J.; Macpherson, J. V.; Unwin, P. R. *J. Phys. Chem. B* **1997**, *101*, 10851.
  - (22) Kwak, J.; Bard, A. J. *Anal. Chem.* **1989**, *61*, 1221.
  - (23) Robinson, R. A.; Stokes, R. H. *Electrolyte Solutions*; Butterworths: London, 1959; pp 491–508.